

# The effect of the rotor elastic anisotropy on the friction drive of the ultrasonic motors

ロータの弾性異方性による超音波モータの摩擦駆動に対する影響の検討

Tatsuki Sasamura<sup>1‡</sup>, Abdullah Mustafa<sup>1</sup>, Susumu Miyake<sup>1</sup>, Norio Sashida<sup>2</sup>, and Takeshi Morita<sup>1</sup>

(<sup>1</sup>Grad. School of Frontier Sciences, The Univ. of Tokyo; <sup>2</sup>SHINSEI CORPORATION)

笹村 樹生<sup>1‡</sup>, Abdullah Mustafa<sup>1</sup>, 三宅 奏<sup>1</sup>, 指田 徳生<sup>2</sup>, 森田 剛<sup>1</sup>

(<sup>1</sup>東大 新領域創成科学研究科, <sup>2</sup>株式会社 新生工業)

## 1. Background

The traveling wave ultrasonic motor (TWUSM) is based on the piezoelectric ultrasonic vibration and frictional contact. While it has significant advantages such as high torque density or fast response, its insufficient efficiency and relatively short lifetime restrict the application area of TWUSM<sup>2)</sup>. Therefore, it is essential to understand its frictional contact to overcome these problems.

The TWUSM model has been studied analytically<sup>2)</sup> or numerically<sup>3)</sup> previously. For example, Storck *et al.* analyzed TWUSM driving characteristics using the analytical model considering the tangential stiffness of the rotor. This research showed the tangential stiffness considerably affects the contact state and efficiency. However, this study only analyzed the commercially available motor, and it is unknown how the design modification affects the frictional contact.

In this study, we simulated the contact force distribution using an analytical model, then evaluated the effect of the rotor stiffness parameters on the frictional contact, such as a change of output torque and driving efficiency.

## 2. Contact model

In this section, we describe the contact model used for the analysis of this research. This model consists of two parts: calculations for the preload distribution and the frictional force distribution.

### 2.1 Preload distribution

The preload applied on the rotor  $F_n$  is distributed on the contact surface as  $f_n(x, t)$ . Therefore, we obtain

$$F_n = \int_0^{2\pi r} f_n(x, t) dx \quad (1)$$

where  $r$  is the effective radius of the contact surface,  $x$  is the position in the circumferential direction,  $t$  is time. In this model, we assume that the preload distribution  $f_n(x, t)$  is proportional to

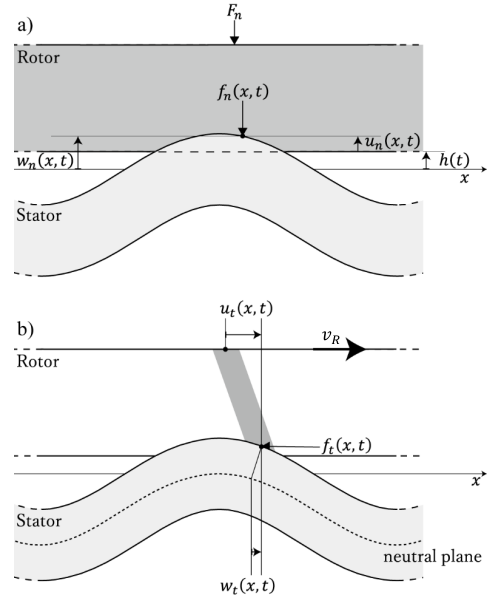


Fig. 1 The contact model of TWUSM. a) Normal direction b) Tangential direction

the normal displacement of the rotor  $u_n(x, t)$ ,

$$f_n(x, t) = c_n u_n(x, t) \quad (2)$$

where  $c_n$  is the normal stiffness.

The rotor contacts the stator and deforms, as shown in **Fig. 1a**. Hence we obtain

$$u_n(x, t) = \begin{cases} w_n(x, t) - h & w_n(x, t) \geq h \\ 0 & w_n(x, t) < h \end{cases} \quad (3)$$

where  $w_n(x, t) = w_{n0} \cos(kx + \omega t)$  is the normal position of the stator,  $h$  is the normal position of the rotor before elastic deformation.

### 2.2 Frictional force distribution

As same as preload distribution, we assumed the frictional force distribution  $f_t(x, t)$  to be proportional to the tangential deformation  $u_t(x, t)$ .

$$f_t(x, t) = c_t u_t(x, t) \quad (4)$$

where  $c_t$  is the tangential stiffness.

The tangential deformation  $u_t(x, t)$  depends on the contact state as stick or slip.

First, the contact surface sticks when  $|f_t(x, t)| < \mu f_n(x, t)$  while  $\mu$  is the frictional coefficient. In this situation, The surfaces of the rotor and the stator

move together at the same speed

$$\frac{\partial u_t}{\partial t}(x, t) + v_R = \frac{\partial w_t}{\partial t}(x, t) \quad (5)$$

where  $v_R$  is the speed of the rotor,  $w_t(x, t)$  is the tangential deformation of the stator. Based on the Bernoulli-Euler assumptions,  $w_t(x, t)$  can be expressed as

$$w_t(x, t) = -a \frac{\partial w_n}{\partial x}(x, t) \quad (6)$$

where  $a$  is the distance between the stator surface and the neutral plane.

Second, when the contact surface slips, we obtain

$$f_t(x, t) = \pm \mu f_n(x, t) \quad (7)$$

while the plus/minus sign depends on the slipping direction. In this case, we can calculate  $u_t(x, t)$  from Eq. 4.

The output torque  $T$ , the output power  $P_{out}$ , the frictional loss  $P_{loss}$ , the efficiency  $\eta$  are calculated below.

$$T = r \int_0^{2\pi r} f_t(x, t) dx \quad (7)$$

$$P_{out} = T v_R / r = v_R \int_0^{2\pi r} f_t(x, t) dx \quad (8)$$

$$P_{loss} = \int_0^{2\pi r} \left( \frac{\partial w_t}{\partial t}(x, t) - v_R \right) f_t(x, t) dx \quad (9)$$

$$\eta = \frac{P_{out}}{P_{out} + P_{loss}} \quad (10)$$

### 3. Analysis of the rotor stiffness effect

We set the rotation speed as 60 rpm and adjusted the vibration amplitude to control the output torque to 0.01, 0.1, 0.3 or 0.6 Nm. Moreover, we changed the normal stiffness  $c_n$  from  $5 \times 10^8$  N/m<sup>2</sup> to  $5 \times 10^{10}$  N/m<sup>2</sup>, and set the tangential stiffness  $c_t$  as  $2.5 \times 10^9$  N/m<sup>2</sup>. The efficiency and the output torque while changing  $c_t$  are shown in **Fig. 2**.

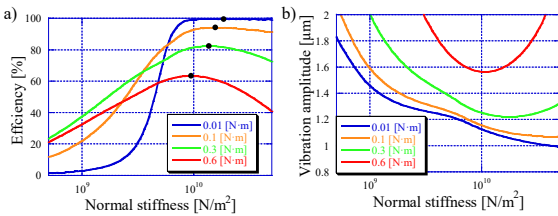


Fig. 2 The characteristics change due to the normal stiffness a) efficiency b) required vibration amplitude (Black points are the point maximizing efficiency.)

Figure. 2a shows that the efficiency curve has maximum value at different stiffness depending on the output torque. When the output torque is low (0.01 Nm), the efficiency is at the maximum with high stiffness and the stiffness at the maximum point decreases by increasing the output torque. Moreover,

when the stiffness is too far from the maximum point, the vibration amplitude for specified torque increased intensely as shown in Fig. 2b.

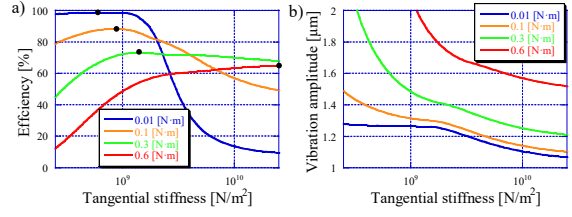


Fig. 3 The characteristics change due to the tangential stiffness a) efficiency b) required vibration amplitude (Black points are the point maximizing efficiency.)

We also simulated the efficiency curve as a function of tangential stiffness  $c_t$  from  $2.5 \times 10^8$  N/m<sup>2</sup> to  $2.5 \times 10^9$  N/m<sup>2</sup> with fixed normal stiffness  $c_n$  at  $5 \times 10^9$  N/m<sup>2</sup> as shown in **Fig. 3**. In contrast to the normal stiffness, the efficiency is high with low stiffness at low torque (0.01 Nm), and the stiffness at the maximum point increases with the larger output torque.

Finally, we changed both normal and tangential stiffnesses shown in **Fig. 4**. At low output torque (0.1 Nm), the efficiency is high with relatively low tangential stiffness comparing with high output torque case (0.5 Nm). This result shows there is an optimum stiffness ratio  $c_t/c_n$  which depends on the output torque.

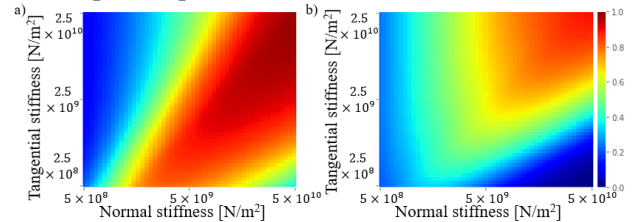


Fig. 3 Color plot of the efficiency as a function of the normal and tangential stiffness with output torque a) 0.1 Nm b) 0.5 Nm

### 4. Conclusion

From the simulation result using the analytical contact model, we found the stiffness of the rotor affects the output performance of TWUSM. Notably, the stiffness parameters have the maximum point which depending on the output torque. With this method, it is possible to design the rotor to maximize frictional efficiency.

### References

1. Z. Chungsheng, "Ultrasonic Motors: Technologies and Applications", 2010.
2. H. Storck, J. Wallaschek, Int. J. Non. Linear. Mech. 38 (2002) 143–159.
3. A. Frangi, A. Corigliano, M. Binci, P. Faure, Ultrasonics. 43 (2005) 747–755.